ON THE ROLE OF SELF-CALIBRATION FUNCTIONS IN INTEGRATED SENSOR ORIENTATION

M. Blázquez and I. Colomina

Institute of Geomatics
Generalitat de Catalunya & Universitat Politècnica de Catalunya
Av. Carl Friedrich Gauss 11
Parc Mediterrani de la Tecnologia, Castelldefels, Spain
marta.blazquez@ideg.es
ismael.colomina@ideg.es

KEY WORDS: calibration, orientation, geometric self-calibration, integrated sensor orientation.

ABSTRACT:

Research on frame camera self-calibration started more than fifty years ago. Its use has become routine and an essential part of camera simultaneous orientation and calibration procedures, even for digital large format cameras as the "Digital Camera Calibration" EuroSDR project has demonstrated. Later, the concept was extended to the geometric calibration of various sensors geometries and to terrestrial and space platforms. Recently, radiometric self-calibration has become a hot research topic. In aerial photogrammetry, there are two main approaches to the modelling of sensor systematic errors; the physical-oriented approach and the numerical-oriented one. The physical oriented approach is best represented by the Conrady-Brown function whereas the numerical oriented one is best represented by the Ebner function or Grün function —whose coefficients constitute the so called 12 Ebner parameter set or 44 Grün parameter set respectively. While the Conrady-Brown function models the von Seidel distortion aberrations, the Ebner function models a general distortion. The Ebner calibration function is a fourth order polynomial built with an orthogonal base whose inner product is related to the standard flight patterns of aerial photogrammetry. Traditionally, the Conrady-Brown function has been applied to close-range photogrammetry and the Ebner function to aerial photogrammetry or, more to the point, to the self-calibrating bundle block adjustment. Because the 12 Ebner set dates back to the mid nineteen seventies and, probably, because of its excellent performance, the fundamental assumptions underneath and the properties of the set have been somewhat forgotten. In the paper, we review some of the principles of the 12 Ebner set, namely that they were derived from a 9 + 9 parameter one and that, from those, 6 parameters were removed to avoid correlations with the exterior orientation parameters in a traditional aerial triangulation configuration; i.e., without GPS and INS aerial control. In the paper we will discuss the case where, for certain aerial control configurations, in the integrated orientation modes, the "missing" 6 parameters in the 12 Ebner set are required. To overcome the limitations of the Ebner self-calibration function, we propose an alternative model and strategy for numerical oriented self-calibration functions valid for both the traditional classical aerial triangulation and the new orientation modes.

1 INTRODUCTION

Sensor calibration is the determination of the parameters $\bar{x}$ of a sensor model $\bar{f}(\ell - e, x, \bar{x}) = 0$ that extends the sensor nominal model $f(\ell - e, x) = 0$. Extending f to $\bar{f}$ can be interpreted as modelling the systematic errors of the sensor. In photogrammetry, the parameters $\bar{x}$ are usually referred to as additional parameters (APs). In photogrammetry and remote-sensing, calibration is invariably applied to every sensor whose accuracy potential has to be met. The calibration concept has several dimensions: sensor and system calibration; temporal, spatial, radiometric and spectral calibration; laboratory, field and self-calibration; physical-oriented and numerical-oriented calibration; etc. Depending on sensor features, the instrumental reference frames of sensors may be temporal, spatial, radiometric and spectral among others. Calibration may be related to all these aspects and even combine them. A comprehensive review of photogrammetric camera calibration for the second half of the past century can be found in (Clarke and Fryer, 1998). A comparative analysis between the concepts of camera calibration in photogrammetry and computer vision can be found in (Remondino and Fraser, 2006).

Calibration may be conducted as a specific, dedicated task either in the laboratory or in the field. Since the parameters determined in a calibration procedure may not remain valid later under different conditions, calibration is also conducted simultaneously to operational data collection tasks. In the latter case, the determination of the calibration parameters $\bar{x}$ is performed simultaneously to the determination of other parameters of interest related to the sensors and systems: the system "calibrates itself" and thus the concept and name "self-calibration." In the former case, the determination of $\bar{x}$ is done "off-line" in a previous, separate and specific procedure. Field calibration is, conceptually, similar to lab calibration where the laboratory environment is replaced by an environment closer to the sensor's operational one.

Self-calibration is a fundamental concept in photogrammetry and remote sensing. The operational method of simultaneous camera orientation and calibration was already

proposed in the mid nineteen sixties (Clarke and Fryer, 1998). It entered the operational workflows of aerial and close-range photogrammetry in the eighties and has survived the transition from film-based analogue photogrammetry to digital photogrammetry. Moreover, the concept of self-calibrating network or block adjustment has been —or more to the point, had to be— adapted to laser scanning.

There are various approaches to geometric camera self-calibration functional modelling. To the risk of being simplistic and of leaving aside other contributions, we recall the two prevailing ones: the physical oriented approach and the numerical oriented one. The physical-oriented approach to tries to understand the various physical causes of sensor systematic errors (like film, optics or CCD-matrix deformations) and to model them. This approach dates back to the nineteen mid fifties and early sixties when the classical physical-oriented lab and self-calibration models for close-range photogrammetry were developed (Brown, 1966, Brown, 1971, Kenefick et al., 1972). These models, that extend the collinearity equations with the so-called self-calibration functions, have been recently applied to the calibration of small- and medium-format cameras on board of aircrafts. They are best represented by the Conrady-Brown self-calibration model.

The numerical-oriented approach acknowledges the complex pattern of image deformations and, rather than understand it, tries to blindly model it with a truncated orthogonal —or numerically well behaved— base of some functional space of $R \times R \longrightarrow R$ functions. Two such functions are then used, for the x and y corrections. This method has been and continues to be instrumental in the accurate orientation and calibration of large-format metric cameras.

An efficient numerical-oriented self-calibration model was proposed in 1976 by Heinrich Ebner in his influential paper (Ebner, 1976). Roughly speaking, it consists of bivariate polynomials $P(x, y)$ of the type

$$P(x, y) = (1, x, x^2)M(1, y, y^2)^T,$$

thus leading initially to 18 (9 + 9) APs and finally to 12 after removing 6 of them to avoid correlations with the sensor exterior orientation (EO) parameters. Heinrich Ebner's model or self-calibration function is usually referred to as the "12 orthogonal Ebner set" or, simply, the "Ebner set" and has become widely used in airborne photogrammetry. (The set was later extended to a 44 parameter one by Armin Grün.) One could say, that the Ebner set is "EO constrained" as it cannot model systematic errors which are equivalent to errors produced by wrong EO parameters.

The Ebner and Grün sets have become so popular that they are being systematically used even when they should not. This papers presents and discusses one such a case. We specifically refer to the situation where the EO parameters are known which is sometimes the case when INS/GPS derived aerial control observations are available.

The paper is organized as follows. In this section we introduce and motivate the present investigation. In section 2 we develop an unconstrained family of self-calibration functions, based on a polynomial orthogonal base, that allow for unconstrained camera calibration when the camera EO parameters are known. The proposed functions contain 9 orthogonal polynomials for the x and y image coordinates, thus leading to an 18 AP set, and are closely related to the "EO constrained" Ebner self-calibration functions. In the same section, we further propose a simple and efficient technique so our unconstrained base can be used when the EO parameters or subsets thereof are known thus avoiding singularities or numerically ill conditioned situations. In section 3 the unconstrained self-calibration base and the adaptation technique are empirically validated by testing them against actual, controlled data sets.

2 COMPLETE SELF-CALIBRATION FUNCTIONS FOR INTEGRATED SENSOR ORIENTATION

The well known Ebner family of self-calibration functions Δx and Δy, parameterized by the 12 coefficients $b_1, \ldots, b_{12}$ (Ebner, 1976), is given by

$$\begin{array}{rcl} \Delta x & = & b_1 x + b_2 y - 2b_3 k + b_4 xy \\ & + & b_5 l + b_7 xl + b_9 yk + b_{11} kl, \\ \Delta y & = & -b_1 y + b_2 x + b_3 xy - 2b_4 l \\ & + & b_6 k + b_8 yk + b_{10} xl + b_{12} kl, \end{array} \tag{1}$$

whose functional base $\{q_i\}_{i=1,\ldots,8}$ consists of the following bivariate polynomials

$$\{x, y, k, xy, l, xl, yk, kl\}$$

where

$$k = x^2 - \frac{2}{3}b^2 \text{ and } l = y^2 - \frac{2}{3}b^2$$

and where b characterizes the 3×3 standard image measurement distribution set $D = \{-b, 0, b\} \times \{-b, 0, b\}$. It can be easily proven that this bivariate polynomial base is orthogonal under the scalar product

$$\langle q_n, q_m \rangle = \sum_{(x,y)\in D} q_n(x, y) \cdot q_m(x, y). \tag{2}$$

In order to construct a complete, unconstrained family of self-calibration functions for the same distribution set D, a natural way to proceed is to start with the Ebner functions and undo the way back to the complete bivariate orthogonal base $\{p_i\}_{i=1,\ldots,9}$ (under the same scalar product (2))

$$\{1, x, y, k, xy, l, xl, yk, kl\}$$

and to the complete family of self-calibration functions parameterized by 18 coefficients

$$\begin{array}{rcl} \Delta x & = & a_{1_1} + a_{2_1} x + a_{1_2} y + a_{3_1} k + a_{2_2} xy + a_{1_3} l \\ & + & a_{2_3} xl + a_{3_2} ky + a_{3_3} kl, \\ \Delta y & = & b_{1_1} + b_{2_1} x + b_{1_2} y + b_{3_1} k + b_{2_2} xy + b_{1_3} l \\ & + & b_{2_3} xl + b_{3_2} ky + b_{3_3} kl. \end{array} \tag{3}$$

Another way to construct the previous self-calibration functions (Grün, 1986) is to consider two univariate orthogonal bases $\{p_i^x\}_{i=1,\dots,3}$ and $\{p_i^y\}_{i=1,\dots,3}$,

$$\{1, x, k\} \text{ and } \{1, y, l\}$$

under similar scalar products related to the point distribution set D

$$\langle p_n^x, p_m^x \rangle = \sum_{i=1,\dots,3} p_n^x(x_i) \cdot p_m^x(x_i), \tag{4}$$

$$\langle p_n^y, p_m^y \rangle = \sum_{i=1,\dots,3} p_n^y(y_i) \cdot p_m^y(y_i) \tag{5}$$

where $x_1 = y_1 = b, x_2 = y_2 = 0, x_3 = y_3 = -b$ and to transform them into complete bivariate self-calibration functions

$$\Delta x = \begin{pmatrix} 1 & x & k \end{pmatrix} \begin{pmatrix} a_{1_1} & a_{1_2} & a_{1_3} \\ a_{2_1} & a_{2_2} & a_{2_3} \\ a_{3_1} & a_{3_2} & a_{3_3} \end{pmatrix} \begin{pmatrix} 1 \\ y \\ l \end{pmatrix},$$

$$\Delta y = \begin{pmatrix} 1 & x & k \end{pmatrix} \begin{pmatrix} b_{1_1} & b_{1_2} & b_{1_3} \\ b_{2_1} & b_{2_2} & b_{2_3} \\ b_{3_1} & b_{3_2} & b_{3_3} \end{pmatrix} \begin{pmatrix} 1 \\ y \\ l \end{pmatrix}.$$

One step more in the generalization of the Ebner self-calibration functions is the extension of the scalar product to rectangular images that lead to the 3×3 image measurement distribution set $D' = \{-b_x, 0, b_x\} \times \{-b_y, 0, b_y\}$. Then, the scalar product (2) becomes

$$\langle p_n, p_m \rangle = \sum_{(x,y) \in D'} p_n(x, y) \cdot p_m(x, y), \tag{6}$$

and the family of bivariate polynomials $\{p_i\}_{i=1,\dots,9}$

$$\{1, x, y, k_x, xy, l_y, xl_y, yk_x, k_x l_y\} \tag{7}$$

where

$$k_x = x^2 - \frac{2}{3} b_x^2 \text{ and } l_y = y^2 - \frac{2}{3} b_y^2$$

is a bivariate orthogonal base under (6) that defines the following complete self-calibration functions

$$\begin{aligned} \Delta x &= a_{1_1} + a_{2_1} x + a_{1_2} y + a_{3_1} k_x + a_{2_2} xy + a_{1_3} l_y \\ &+ a_{2_3} x l_y + a_{3_2} k_x y + a_{3_3} k_x l_y, \\ \Delta y &= b_{1_1} + b_{2_1} x + b_{1_2} y + b_{3_1} k_x + b_{2_2} xy + b_{1_3} l_y \\ &+ b_{2_3} x l_y + b_{3_2} k_x y + b_{3_3} k_x l_y. \end{aligned} \tag{8}$$

Note that the complete self-calibration functions for square images given in (3) are a particular case of the complete self-calibration functions for rectangular images just defined in (8) with $b_x = b_y = b$.

Self-calibration functions (1) —the Ebner model parameterized by 12 coefficients— were designed for Indirect Sensor Orientation (InSO); i.e., the old aerial triangulation with neither GPS nor INS/GPS aerial control. Self-calibration functions (8) —this paper's model parameterized by 18 coefficients— are designed for Integrated Sensor Orientation (ISO); i.e., modern aerial triangulation with INS/GPS aerial control. The main difference between functions (1) and (8) is the number of coefficients or, in other words, the number of APs to be estimated in the block adjustment. In (8) there are six more coefficients —unknown parameters— than in (1) which may be an advantage as well as a disadvantage. It is an advantage when the INS/-GPS derived position and attitude are accurate and the sensor system is calibrated. It is a disadvantage when the INS/GPS derived position and attitude are affected by systematic errors like GPS shifts or when the camera-to-IMU relative attitude parameters are unknown. In these two cases, unknown GPS shifts or camera-to-IMU attitude, the use of the complete self-calibration functions (8) will lead to numerical instabilities or singularities. On the contrary, if the INS/GPS aerial control is accurate and if the camera-to-IMU attitude is known from a previous system calibration step, the use of the Ebner self-calibration functions (1) will lead to suboptimal results.

The situation described above may look hopeless in that there are no self-calibration functions that can cope with the various configurations and aerial control models (Blázquez, 2008) of today's blocks. However, we claim that the complete functions (8) can be used for all configurations if appropriate constraints for some of the 18 APs are imposed. From the analysis of the correlations between the calibration parameters and from the close relationship between equations (1) and (8), we propose the following constraints to avoid the correlations between the complete self-calibration parameters with the EO position parameters (or the GPS shift parameters) and also with the EO attitude parameters (or the camera-to-IMU attitude parameters).

- With the X, Y components:

$$a_{1_1} = b_{1_1} = 0.$$

- With the Z component:

$$a_{2_1} + b_{1_2} = 0.$$

- With the ω component:

$$b_{1_3} + 2a_{2_2} = 0. \tag{9}$$

- With the ϕ component:

$$a_{3_1} + 2b_{2_2} = 0.$$

- With the κ component:

$$a_{1_2} - b_{2_1} = 0.$$

In short, we propose to use the complete self-calibration functions (8) for both square and rectangular images, for both ISO and InSO modes with the appropriate previous constraints.

3 CONCEPT VALIDATION RESULTS

The goal of this section is to validate the alternative complete self-calibration functions presented in the previous section. To analyse the overall feasibility and validate the concept, the complete self-calibration functions are tested against the Ebner self-calibration ones with different data sets (section 3.1) and configurations (section 3.2). The results of this investigation are presented in sections 3.3 and 3.4.

3.1 Data sets description

Two data sets have been used: the "Pavia block" and the "Vaihingen/Enz gsd7 block." The configuration characteristics of the Pavia block are summarized in table 1 and its layout can be seen in figure 1. The configuration characteristics of the Vaihingen/Enz gsd7 block are summarized in table 2 and its layout can be seen in figure 2.

Figure 1: Pavia block layout.

Equipment	RC30 GPS antenna + IMU
Scale	1:8000
Flying height	1200 m
Gsd	11 cm
No. of strips	11 (7+4)
No. of images per strip	≈ 10
No. of photo-observations per image	≈ 30
No. of Ground Control Points (GCP)	8
No. of Ground Check Points (CP)	25
No. of images	131
No. of photo-observations	4167
No. of tie-points	478
Overlap	$\approx 60\% \times 60\%$
Coordinate reference frame	3D local cartesian

Table 1: Pavia block characteristics.

3.2 Tests configurations

Just as with the Ebner self-calibration functions, the complete self-calibration functions are added to the collinearity equations in a general network adjustment software. Due to the different coordinate reference frames of the available data sets, the complete self-calibration functions are combined with the collinearity equations in a 3D local cartesian coordinate reference frame (l-CRF) and a 3D-hybrid (2D-map projection and 1D-height) coordinate reference frame (m-CRF).

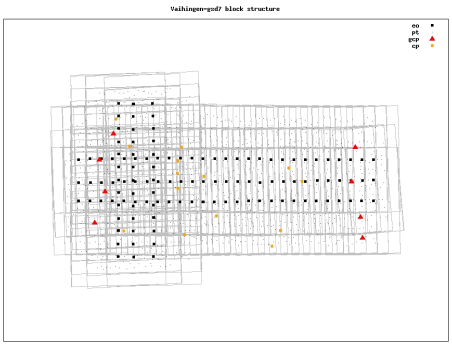

Figure 2: Vaihingen/Enz gsd7 block layout.

Equipment	Dual-DigiCAM-H/39 GPS antenna + IMU
Scale	1:14000
Flying height	1150 m
Gsd	9.5 cm
No. of strips	6 (3+3)
No. of images per strip	≈ 20 x 2
No. of photo-observations per image	≈ 30
No. of Ground Control Points (GCP)	8
No. of Ground Check Points (CP)	14
No. of images	120 x 2
No. of photo-observations	7910
No. of tie-points	1106
Overlap	$\approx 60\% \times 76\%$
Coordinate reference frame	3D-hybrid (map projection + H)

Table 2: Vaihingen/Enz gsd7 block characteristics.

The selected and most representative configurations of the performed tests are described in table 3.

Test	Self-calibration functions	GPS shift linear parameter	Camera-to-IMU angular parameter
A	Ebner	none	known
B	Ebner	1 shift/block	unknown
C	Ebner	1 shift/strip	unknown
D	Complete	none	known
E	Complete	1 shift/block	unknown
F	Complete	1 shift/strip	unknown

Table 3: Test configurations.

These tests are characterised by the use of different self-calibration functions, the configuration of the GPS shift linear parameter and the configuration of the camera-to-IMU angular parameter. In the case of self-calibration functions, the proposed complete self-calibration functions (equations (8)) are compared with the Ebner ones (equations (1)). In the case of the GPS shift parameter, three options are available: no GPS shift parameter, one free GPS shift parameter per block and one free GPS shift parameter per strip. With respect to the camera-to-IMU angular parameter (boresight parameter group), two configurations are available: the parameter group is known (the known value is introduced in the adjustment as a constant) or the parameter group is unknown (its value is computed in the network adjustment).

As it is well known, the usual workflow for ISO consists of

computing exterior orientation and tie point parameters in a network adjustment, where the observations are the measured image coordinates, the coordinates of few ground control points and the INS/GPS derived position and attitude observations. In the same adjustment the GPS shift and camera-to-IMU parameters are computed. This configuration corresponds to the tests B, C and E, F.

3.3 Pavia block results

In the case of the Pavia block, for all configurations, the observables' precisions at the 1-σ level are listed in table 4.

Observable	Precision	Units
Image coordinates	$\sigma_x = \sigma_y = 4.8$	μm
Ground control points	$\sigma_X = \sigma_Y = 8 \quad \sigma_Z = 10$	cm
INS/GPS-position	$\sigma_X = \sigma_Y = 3.5 \quad \sigma_Z = 5.5$	cm
INS/GPS-attitude	$\sigma_r = \sigma_p = 18 \quad \sigma_h = 28.8$	”

Table 4: Pavia block observables' precisions.

Table 5 shows the absolute accuracy from check points (CP) and precision from tie points (TP) for the different tests with the Pavia block data set. Table 6 shows the precision from exterior orientation parameters (EO) for the different tests with the Pavia block data set.

	Accuracy RMS CP (cm)			Precision MEAN σ TP (cm)		
Test	X	Y	Z	X	Y	Z
A	3.55	2.87	23.84	2.27	2.40	3.98
B	3.31	2.41	3.47	3.65	3.74	5.37
C	3.59	2.71	3.19	3.57	3.66	5.26
D	3.58	2.63	3.10	2.20	2.34	5.18
E	3.31	2.41	3.47	3.65	3.74	5.37
F	3.59	2.71	3.19	3.57	3.66	5.26

Table 5: Pavia block CP and TP results.

	Precision MEAN σ EO (cm/”)					
Test	X	Y	Z	ω	ϕ	κ
A	2.58	2.59	1.78	3.92	3.99	2.78
B	3.81	3.82	4.04	3.91	3.98	2.77
C	3.86	3.93	3.96	4.10	4.01	2.74
D	2.52	2.53	1.73	4.08	4.15	3.63
E	3.81	3.82	4.09	3.91	3.98	2.96
F	3.86	3.94	4.00	4.11	4.01	2.92

Table 6: Pavia block EO results.

As expected, for the most common configurations (B, C, E, F) tables 5 and 6 demonstrate that the results are equivalent if the used self-calibration functions are the Ebner or the complete ones adding constraints (9) to avoid the correlations between the self-calibration parameters and the position and attitude parameters (GPS shift and camera-to-IMU attitude).

Tables 5 and 6 validate the proposed concept for the complete self-calibration parameters with the tests, A and D, where the position parameter, GPS shift, is not taken into account in the adjustment and the camera-to-IMU attitude parameter is known and introduced in the adjustment as a constant. As it can be seen in figure 3, if the self-calibration parameters used in the adjustment are the Ebner ones, test A, the check points are affected by a shift in the Z component of more than 20 cm. In fact, in the configurations B, C, E, F, where the GPS shift parameter is adjusted, the value of this parameter group in the Z component is around 20 cm. However, the results of test D (figure 4) show that the complete 18 parameters are able to absorb this shift in the Z component even the GPS shift parameter is not considered.

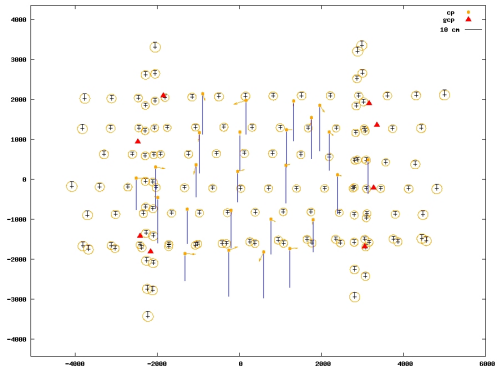

Figure 3: Pavia block test A results.

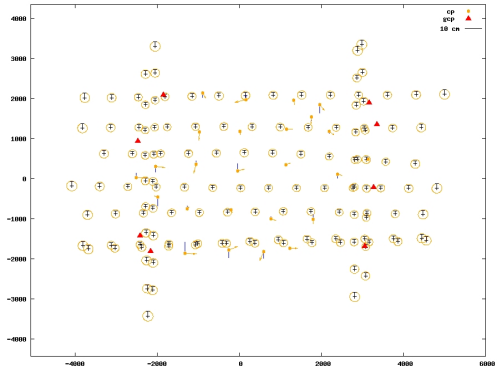

Figure 4: Pavia block test D results.

3.4 Vaihingen/Enz gsd7 block results

In the case of the Vaihingen/Enz gsd7 block, for all the configurations, the observables' precisions at the 1-σ level are listed in table 7.

Observable	Precision	Units
Image coordinates	$\sigma_x = \sigma_y = 1.4$	μm
Ground control points	$\sigma_X = \sigma_Y = \sigma_Z = 2$	cm
INS/GPS position	$\sigma_X = \sigma_Y = 3.5 \quad \sigma_Z = 5.5$	cm
INS/GPS attitude	$\sigma_r = \sigma_p = 18 \quad \sigma_h = 28.8$	”

Table 7: Vaihingen/Enz gsd7 block observables' precisions.

For this data set, the camera system is a Dual-DigiCAM-H3C9 (Kremer and Cramer, 2008). Therefore, for all the configurations a model that relates the position and attitude of one of the DigiCAM-H39 camera to the other one is added to the collinearity equations with the self-calibration functions and position and attitude aerial control model in the adjustments.

Table 8 shows the absolute accuracy from check points (CP) and precision from tie points (TP) for the different

tests with the Vaihingen/Enz gsd7 block data set. Table 9 shows the precision of EO parameters for the various tests with the Vaihingen/Enz gsd7 block data set.

	Accuracy RMS CP (cm)			Precision MEAN σ TP (cm)		
Test	X	Y	Z	X	Y	Z
A	1.85	3.04	5.41	1.21	1.63	3.94
B	1.97	2.43	5.83	1.46	1.83	4.07
C	1.84	2.46	6.15	1.47	1.84	4.06
D	1.83	3.08	5.54	1.21	1.63	4.04
E	1.97	2.43	5.83	1.46	1.83	4.07
F	1.84	2.46	6.14	1.47	1.84	4.06

Table 8: Vaihingen/Enz gsd7 block CP and TP results.

	Precision MEAN σ EO (cm/")					
Test	X	Y	Z	ω	ϕ	κ
A	1.92	1.80	1.24	4.25	4.51	3.32
B	2.15	2.04	1.85	4.60	4.83	3.37
C	2.31	2.23	1.87	4.85	5.00	3.38
D	1.91	1.79	1.24	4.29	4.56	3.70
E	2.15	2.04	1.88	4.60	4.83	3.52
F	2.31	2.23	1.89	4.85	5.00	3.53

Table 9: Vaihingen/Enz gsd7 block EO results.

Similarly to the Pavia block, tables 8 and 9 demonstrate that for the most common configurations, tests B, C, E and F, the results are equivalent if the used self-calibration functions are the Ebner or the complete ones with constraints.

Unlike the Pavia block, for the Vaihingen/Enz gsd7 block, the results of tests A and D (figures 5 and 6), where the GPS shift parameter is not considered and the camera-to-IMU parameter is constant, are equivalent if the self-calibration parameters used in the adjustment are the Ebner ones or the proposed complete ones. In this case, in the configurations B, C, E, F, where the GPS shift parameter is adjusted, the value of this parameter group is not significant. Therefore there is no shift to absorb with the six additional parameters of the complete self-calibration functions.

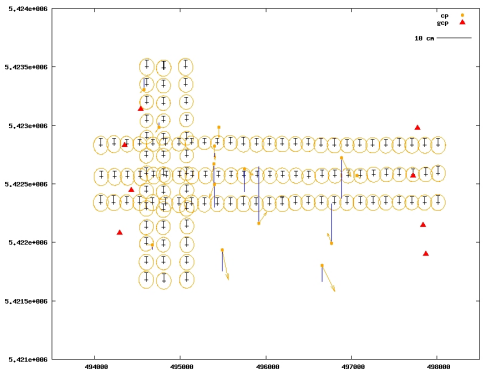

Figure 5: Vaihingen/Enz gsd7 block test A results.

4 CONCLUSIONS AND FURTHER RESEARCH

We have proposed a 18 additional parameter self-calibration function (8) that is based on an orthogonal base (7) and

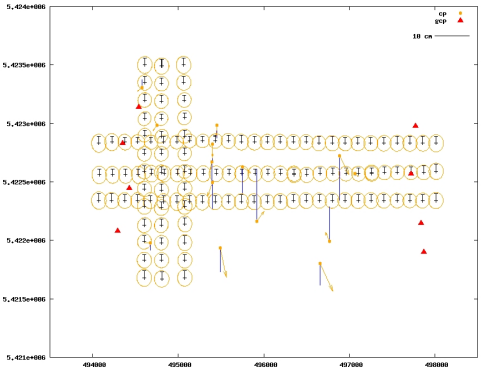

Figure 6: Vaihingen/Enz gsd7 block test D results.

that, together with a set of six selectable constraints (9), generalizes the Ebner 12 parameter self-calibration functions (1). It can be applied to rectangularly shaped images, to classical aerial triangulation (InSO) and to the various control and parameter configurations of ISO. We have evaluated the performance of the new function and shown that, for those situations where the Ebner self-calibration function is adequate, the same results are obtained. It is straightforward to extend the new self-calibration function to a 50 additional parameter function that generalize the Grün's 44 parameter self-calibration one for 5 $\times$ 5 image measurement schemes.

Our next research in this area will concentrate on the development of self-calibration functions for general image measurement distributions and on general, automatic ways to avoid overparameterization regardless of the control configurations.

5 ACKNOWLEDGEMENTS

The research reported in this paper has been funded by the projects LIRA (Ref. P 44/08, Ministerio de Fomento, Spain) and GeoLandModels (Ref. PET2008_071, Ministerio de Ciencia e Innovación, Spain). The models were designed, implemented and tested by the authors and run on the network adjustment platform GENA from GeoNumerics (Barcelona, Spain). The block data set of Pavia was made available by Prof. Vittorio Casella (Università di Pavia, Italy). The block data set of Vaihingen/Enz gsd7 was made available by Dr. Jens Kremer (IGI Ingenieurgesellschaft für Interfaces mbH, Kreuztal, Germany) and Dr. Michael Cramer (Institut für Photogrammetrie, Universität Stuttgart, Germany).

REFERENCES

Blázquez, M., 2008. A new approach to spatio-temporal calibration of multi-sensor systems. In: International Archives of Photogrammetry, Remote Sensing and Spatial Information Sciences, Vol. 37(Part B1), Beijing, China.

Brown, D., 1966. Decentering distortion of lenses. Photogrammetric Engineering 32(3), pp. 444–462.

Brown, D., 1971. Close range camera calibration. Photogrammetric Engineering 37(8), pp. 855–866.

Clarke, T. and Fryer, J., 1998. The development of camera calibration methods and models. Photogrammetric Record 16(91), pp. 51–66.

Ebner, H., 1976. Self calibrating block adjustment. In: International Archives of Photogrammetry, International Society for Photogrammetry and Remote Sensing, Helsinki, Finland.

Grün, A., 1986. Photogrammetrische Punktbestimmung mit der Bündelmethode. Mitteilungen, Vol. 40, Institut für Geodäsie und Photogrammetrie, ETHZ, Zürich, Switzerland.

Kenefick, J., Gyer, M. and Harp, B., 1972. Analytical self-calibration. Photogrammetric Engineering 38(11), pp. 1117–1126.

Kremer, J. and Cramer, M., 2008. A new approach to spatio-temporal calibration of multi-sensor systems. In: International Archives of Photogrammetry, Remote Sensing and Spatial Information Sciences, Vol. 37(Part B1), Beijing, China.

Remondino, F. and Fraser, C., 2006. Digital camera calibration methods: considerations and comparisons. In: International Archives of Photogrammetry and Remote Sensing, Vol. 36(Part B5), Dresden, Germany.